Correlative transmission electron microscopy and electrical properties study of switchable phase-change random access memory line cells

Oosthoek, J. L. M.; Voogt, F. C.; Attenborough, K.; Hurkx, G. A. M.; Gravesteijn, D. J.; Kooi, B. J.

Published in:
Journal of Applied Physics

DOI:
10.1063/1.4908023

Publication date:
2015

Correlative transmission electron microscopy and electrical properties study of switchable phase-change random access memory line cells

J. L. M. Oosthoek, F. C. Voogt, K. Attenborough, M. A. Verheijen, G. A. M. Hurkx, D. J. Gravesteijn, and B. J. Kooi

Citation: Journal of Applied Physics **117**, 064504 (2015); doi: 10.1063/1.4908023
View online: https://doi.org/10.1063/1.4908023
View Table of Contents: http://aip.scitation.org/toc/jap/117/6
Published by the American Institute of Physics

Correlative transmission electron microscopy and electrical properties study of switchable phase-change random access memory line cells

J. L. M. Oosthoek,[1] F. C. Voogt,[2] K. Attenborough,[2] M. A. Verheijen,[3,4] G. A. M. Hurkx,[5] D. J. Gravesteijn,[6] and B. J. Kooi[1,a)]

[1]*Zernike Institute for Advanced Materials and Materials innovation institute M2i, University of Groningen, Nijenborgh 4, 9747 AG Groningen, The Netherlands*
[2]*NXP, Gerstweg 2, 6534 AE Nijmegen, The Netherlands*
[3]*Department of Applied Physics, Eindhoven University of Technology, NL-5600 MB Eindhoven, The Netherlands*
[4]*Philips Innovation Services Eindhoven, High Tech Campus 11, NL-5656 AE Eindhoven, The Netherlands*
[5]*NXP Semiconductors, High Tech Campus 60, 5656 AE Eindhoven, The Netherlands*
[6]*NXP Semiconductors, Kapeldreef 75, B 3001 Leuven, Belgium*

(Received 15 September 2014; accepted 2 February 2015; published online 10 February 2015)

Phase-change memory line cells, where the active material has a thickness of 15 nm, were prepared for transmission electron microscopy (TEM) observation such that they still could be switched and characterized electrically after the preparation. The result of these observations in comparison with detailed electrical characterization showed (i) normal behavior for relatively long amorphous marks, resulting in a hyperbolic dependence between SET resistance and SET current, indicating a switching mechanism based on initially long and thin nanoscale crystalline filaments which thicken gradually, and (ii) anomalous behavior, which holds for relatively short amorphous marks, where initially directly a massive crystalline filament is formed that consumes most of the width of the amorphous mark only leaving minor residual amorphous regions at its edges. The present results demonstrate that even in (purposely) thick TEM samples, the TEM sample preparation hampers the probability to observe normal behavior and it can be debated whether it is possible to produce electrically switchable TEM specimen in which the memory cells behave the same as in their original bulk embedded state. © *2015 AIP Publishing LLC*. [http://dx.doi.org/10.1063/1.4908023]

INTRODUCTION

After being a success in rewritable optical disk technology, well-known from the CD, DVD, and BluRay Disk formats, phase-change materials also appear to have a bright future in fully electrical solid-state memory mainly to replace the currently popular Flash memory.[1–4] Still, for this so-called Phase-change Random Access Memory (PRAM) to become a robust memory technology, reliability issues have to be addressed, which require an improved understanding of the relationship between nanostructure and the properties of actual PRAM cells. A suitable technique for establishing this relation is Transmission Electron Microscopy (TEM). Ideally, the electrical switching and characterization are combined employing *in situ* TEM observations. Recent examples of this approach, although not applied to actual memory cells, are provided in Refs. 5–8. However, the disadvantage of such a direct approach is that locally the PRAM cell (i.e., the layers above and below the active phase-change medium) has to be thinned to a typical thickness of 100 nm in order to allow for TEM imaging. This reduced thickness generally alters the thermal properties and thereby also the electrical properties of the PRAM cells, i.e., the cells in a memory will not behave the same as the *in situ* analyzed cells. In order to avoid these effects we performed in a previous work electrical characterization on real memory cells and brought these cells to certain well defined final states and then prepared (locally thinned) the cells such that they could be analyzed by TEM.[9] In this way, we were able to establish and understand nanostructure property relations for actual memory cells.

In the present work, we focus on the same line cell memories that can be imaged in the TEM, but now they can be still switched and characterized electrically and thus include the drawback of the altered properties due to thinning of the actual memory. It is shown that, despite the large thickness of the TEM samples used to minimize changes in thermal environment, which leads to TEM images with deteriorated resolution and contrast, still the behavior for such a memory cell in a thinned TEM sample is not the same as for the original cell in the bulk. This also shows that work performed such as in Ref. 7 on thin samples is of limited value for actual memory cells. Moreover, earlier *in situ* electrical switching TEM studies of phase-change materials all concentrated on the most popular phase change material $Ge_2Sb_2Te_5$,[4–8] that can be typified as a nucleation dominant material.[10,11] In contrast, here we analyze a so-called fast-growth type material, i.e., (Ge,In) doped SbTe alloy. Thermal erasure of an amorphous mark in this type of material does not depend on nucleation, but only on (re)growth from the crystalline rim. However, during electrically driven erasure, after threshold switching, crystalline filaments are expected to play a crucial role.

Extensive electrical characterization of these line cells has been performed (see, e.g., Refs. 2, 12–17) and also to

a)Author to whom correspondence should be addressed. Electronic mail: B.J.Kooi@rug.nl

much lesser extent TEM images have been recorded of *post mortem* PRAM line cells (see, e.g., Refs. 9, 12, and 18). The main motivation to pursue this goal of observing *in situ* switchable PRAM cell is that correlative studies of TEM imaging and electrical switching and characterization of PRAM line cells are lacking. Still, for answering many open questions concerning PRAM cells, correlative research on switchable PRAM TEM samples is required. The great potential of this approach has been demonstrated recently for phase-change nanowires.[8]

To give a few examples of open questions: (1) It is still not fully known how the amorphous mark is erased during the crystallization pulse, i.e., if nanoscale crystalline filaments are formed first or that the crystallization front proceeds uniformly or in another manner. (2) Cyclability of the memory is limited by decomposition of the phase-change material (PCM) and by electromigration. These processes are not properly observed and understood for nanoscale PCM cells.[9,16,19–24] (3) The transformation from the crystalline to the amorphous phase is associated with a volumetric expansion of about 6%.[25,26] Since the phase-change material is completely encapsulated, this volumetric expansion will create large stresses within the PCM. In return, these stresses influence the crystallization process; this is not properly understood.[27,28] (4) The relations between amorphous mark length and resistance or threshold voltage tend to be proportional, but for detailed studies of these relations correlative research on switchable PRAM TEM samples is needed.[9,16] The present work contributes to answering questions 1 and 4.

RESULTS AND DISCUSSION

PRAM line cells, where the active phase-change material has a thickness of 15 nm, were processed using Focused Ion Beam (FIB) systems (see electronic supplementary information[30] for the details) in such a way that they could be observed in the TEM and still could be switched and characterized electrically. An overview light microscopy image of such a prepared cell is show in Figure S4 of the supplementary information,[30] indicating the locally thinned region around the line cell and the two bond pads that were used for making the electrical connection. Note that the FIB preparation was performed in various steps (see supplementary information[30]), where in a first step the Si substrate was removed completely over a large area also underneath the bond pads. This made it difficult to contact the bond pads with a probe system without puncturing the thin membrane. Still, relevant switching experiments could be performed on such a line cell where the electrical properties could be correlated with TEM images. In order to understand the results, the overview TEM image shown in Figure 1(a) is required. It shows that the line cell still has proper electrical contacts on both sides, but these metallic contacts as imaged black in the TEM image show 90° turn connections only towards the upper side in the image. The analogous 90° turn connections which should be observable at the lower side in the image are absent, because apparently they have been removed during the FIB process only leaving at this location a thin SiO_2 region. This makes the electrical connection to the line cell

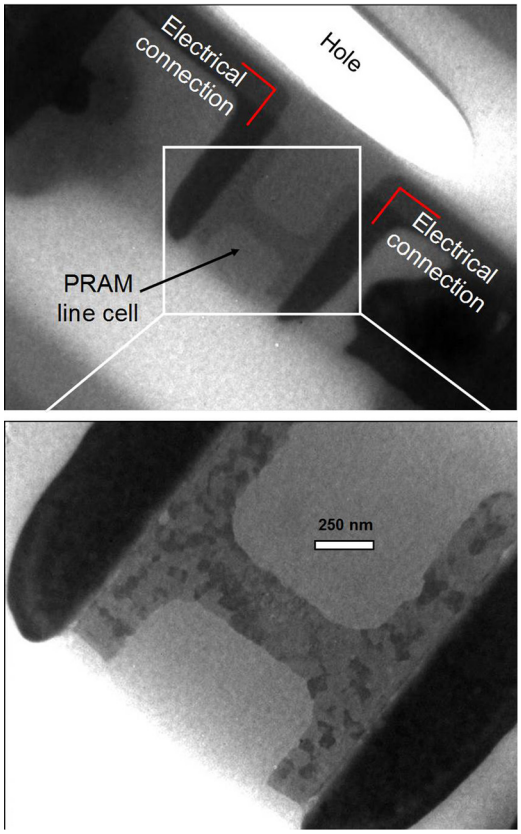

FIG. 1. Top: Overview TEM image showing faintly the dog-bone shaped PRAM line cell in the middle still being electrically connected on both sides by the black metallic contacts (showing a 90° turn at the upper side as highlighted by the overlaid red lines with mutual 90° angle). The brightest area on top shows as indicated a hole made by the FIB process. Also on the lower left side a relatively bright area can be discerned which correspond to a thin region, where the FIB process has actually completely removed the 90° turns of the runners on the lower side making the electrical connection quite asymmetric. Bottom: More detailed bright-field TEM image of the PRAM line cell showing crystalline contrast in phase-change material throughout the line cell indicating that it is in the SET state. A relatively defocused electron beam with long exposure times of 20 s was needed to obtain sufficient contrast without damaging the line cell by the incident energetic (200 kV) electrons.

asymmetric. Another asymmetry that can be observed in the image is that a hole is present only near the top side of the image (most bright region).

Figure 2 summarizes the central results, i.e., showing TEM images for a switching experiment allowing a unique direct correlation between TEM images and electrical characterization and switching. The contrast is limited, because only a 15 nm phase-change film is present in a sample with a total thickness near to 200 nm. Fig. 2(a) image shows the initial state of the cell after preparation indicating that the cell is in the fully crystalline SET state. This is in agreement with the measured resistance of the cell of 2.0 kΩ (reading voltage 0.2 V). This resistance is about the same as the one measured for line cells in the original (thick) memory. Fig. 2(b) shows the structure of the line cell after a 50 ns 4.8 V RESET pulse was applied. It can be observed that this pulse successfully produced an amorphous mark (outlined blue) in the cell. However, another interesting feature can be observed, because the comparison between Figs. 2(a) and 2(b) indicates that a much larger part of the line cell was molten during the RESET pulse (blue + red regions). The

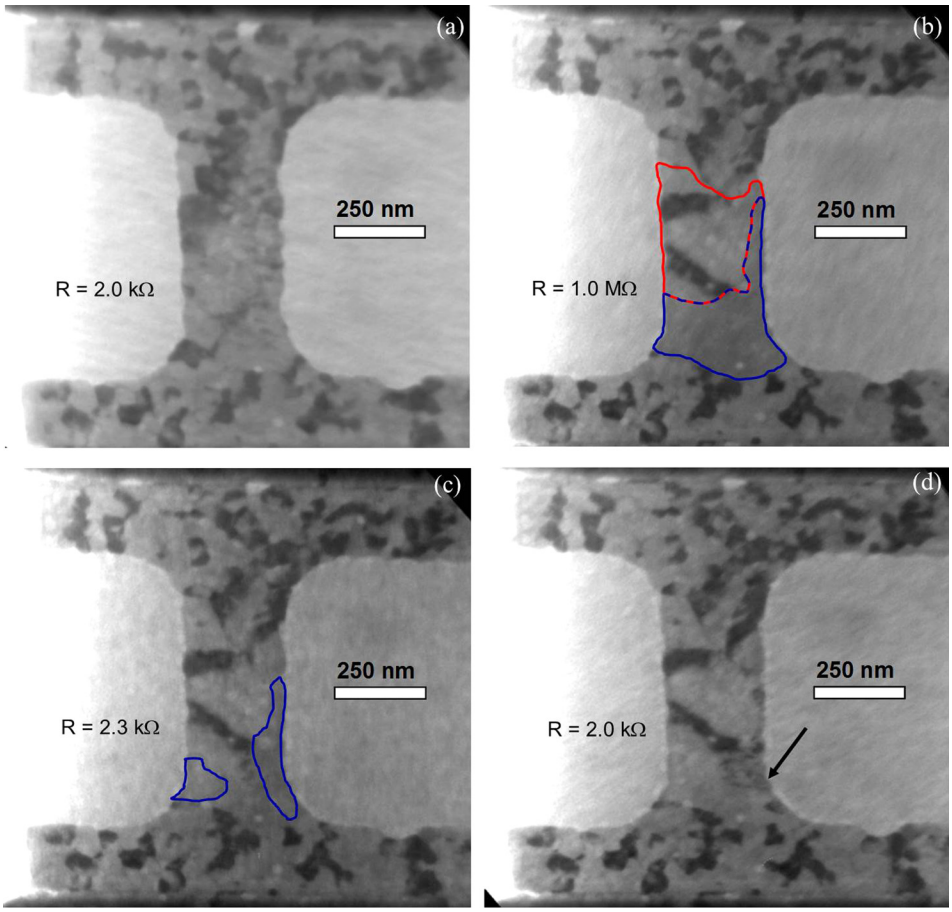

FIG. 2. Correlation of TEM images and electrical characterization and switching. (a) The initial SET state (fully crystalline, 2.0 kΩ). (b) The image shows the structure after a 50 ns 4.8 V RESET pulse, indicating the amorphous mark (outlined blue), the region that was molten during the SET pulse (blue + red regions) and the region that recrystallized during cooling (outlined red). The corresponding resistance is 1.0 MΩ. (c) The image shows again the SET state after a 200 ns 2.8 V pulse giving a resistance of 2.3 kΩ, but still residual amorphous regions (outlined blue) are present. (d) The image shows the subsequent SET state after a series of 200 ns pulses, with voltages increasing to 4 V as shown in Fig. 3, which removed the residual amorphous regions, decreasing the resistance from 2.3 to 2.0 kΩ. The arrow in the bottom-right image points at a region that has been crystallized during the series of 200 ns pulses.

region outlined red must have been recrystallized during (insufficiently fast) cooling. The corresponding resistance of the line cell with the amorphous mark (outlined blue) is 1.0 MΩ. This resistance value, that is 500 times larger than of the initial SET state, indeed proves that an amorphous mark must be present, but this value is about a factor 5 to 10 lower than the RESET resistance normally measured for the same line cells in a memory that has not been thinned for TEM imaging. This demonstrates that the amorphous mark is much smaller than usual and corroborates the observation that a larger part of the line cell was molten but also recrystallized due to slower cooling.

The reason that a smaller amorphous mark is obtained than the region molten during the RESET pulse is straightforward. Due to the FIB preparation, most of the volume surrounding the line cell has been removed and therefore the heat produced in the line cell due to Joule heating during the RESET pulse cannot be conducted as effective to the surroundings as in a normal thick memory. Therefore, the cooling is not as fast as in the original memory. This effect in combination with the extremely high crystal growth rates that are possible in this so-called fast-growth PCM allows recrystallization in a part of the molten region. This process results in a shorter amorphous mark and a lower resistance than observed usually for the cells in a thick memory. Still, an interesting feature is that this recrystallized part has an asymmetric position that is in accordance with the asymmetric configuration of the electrical connection by the runners as was explained above. It is also evident that the hole produced by the FIB (cf. Fig. 1(a)) is not relevant, because heat can still be conducted effectively along the hole by the runners. Therefore, it may be concluded that the PRAM line cell operation is not seriously affected when most of the volume surrounding the line cell is removed by FIB as long as the complete electrical connection to the line cell is preserved and not damaged by the FIB process.

The amorphous mark observable in the Fig. 2(b) could be erased by a 200 ns 2.8 V SET pulse, i.e., the observed threshold voltage was 2.8 V. The result of this operation is shown in Fig. 2(c). The corresponding line cell resistance was 2.3 kΩ, somewhat higher than the 2.0 kΩ resistance of the initial SET state shown Fig. 2(a). Indeed, careful inspection of the TEM image shows that the amorphous mark is not completely erased and that still residual amorphous regions (outlined blue) are present. Another interesting result that can only be obtained by correlating TEM images with the observed threshold voltage is that the more relevant material specific threshold field can be determined. In order to do so, the threshold voltage has to be divided by the amorphous mark length, which is generally unknown, but now can be directly measured in the TEM image (Fig. 2(b)). The observed length is 250 ± 20 nm giving a threshold field of 11 ± 1 V/μm. In our previous work for the same PCM, a threshold field of 26 ± 2 V/μm was determined.[9] In the seminal work by Lankhorst *et al.*,[2] a threshold field for the same PCM of 14 V/μm was derived, but their data show that for short line cells the threshold field seems higher than for long ones (ranging between 20 and 10 V/μm). This indeed also

seems to hold in our case, because in our previous work[9] the line cells examined had a length of 225 nm and in this chapter the length of the line cells is 800 nm. The threshold field was determined by Krebs *et al.*[29] for various materials giving the following values (in V/μm): 8.1 ± 0.2 for $Ge_{15}Sb_{85}$, 19 ± 1 for AgInSbTe alloy, and 56 ± 2 for $Ge_2Sb_2Te_5$. The present GeInSbTe alloy is most similar to their AgInSbTe alloy merely replacing the same amount of Ag by Ge and indeed the threshold fields determined in our work are also close to their value. It might be possible that the threshold field of a PCM is lowered by the defects created in the PCM during the final stages of the FIB process and even by the damage created during TEM imaging by irradiation with 200 kV electrons, where we observed (see supplementary information[30]) that severe damage to the line cells can be easily created. Unfortunately, we were not able to test this hypothesis of electron irradiation lowering of the threshold field. The result in an earlier *in-situ* TEM study[7] seems to hint in this direction, because a threshold field for $Ge_2Sb_2Te_5$ as low as 4 V/μm was observed, which is an order of magnitude lower than mentioned above.[2,29] First of all in Ref. 7 very long (>1 μm) line cells are analysed which will lower the threshold field (by not more than a factor 2), but more important is that they analysed their amorphous marks by TEM, before they applied the threshold voltage and this may have led to a further reduction in threshold field.

Since the SET state shown in Fig. 2(c) still contains some residual amorphous regions a series of 200 ns, SET pulses was applied with voltages increasing from 1 V to 4 V in steps of 0.1 V. The measured line cell resistances as a function of the voltage of these SET pulses are shown in Figure 3. It can be observed in Fig. 3 that for pulses in-between 1.0 and 2.6 V, the resistance remains at the initial 2.3 kΩ value. For pulses in-between 2.6 and 4.0 V, a gradual decrease of the resistance to 2.0 kΩ can be observed in Fig. 3 and this is not altered anymore for pulses higher than 4.0 V. Indeed, the value of 2.0 kΩ corresponds to the initial fully crystalline SET state shown in Fig. 2(a). Fig. 2(d) shows the TEM image after this complete series of 200 ns pulses (with voltages increasing to 4 V) was applied. As expected, the residual amorphous regions were removed by the series of pulses. The arrow in the bottom-right image points at such a region that has been crystallized during the series of 200 ns pulses.

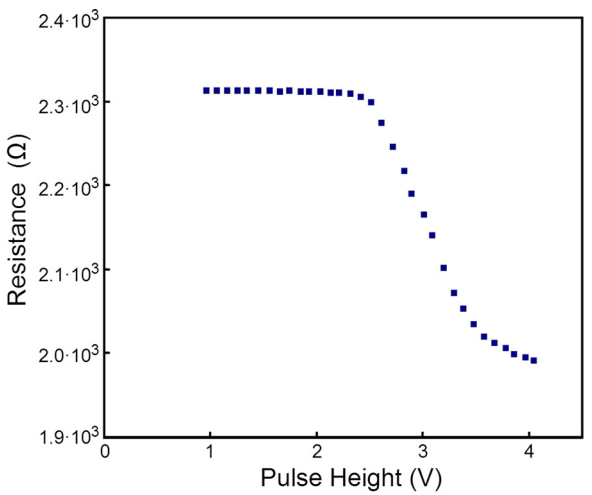

FIG. 3. Development of resistance of the line cell shown in Fig. 2(c) (bottom left) towards to the one shown in Fig. 2(d) (bottom right) by a series of 200 ns pulses, with voltages increasing from 1 to 4 V in steps of 0.1 V.

It would be of great interest to repeat the complete switching cycle shown in Fig. 2 several times in order to obtain statistics and to repeat it for various line cells (e.g., with different lengths). Unfortunately, this was not possible, because the preparation method with complete removal of the Si substrate also below the bond pads made it nearly impossible to contact these pads by probe needles without destroying the sample. Still, a final interesting comparison between the results obtained in Figs. 2 and 3 and independent electrical characterization results of original PRAM cells showing much better statistics, see Figure 4, can be made. The results of Fig. 4 hold for 700 nm long line cells and show the development of the SET resistance when SET pulses with gradually increasing currents are used. Two types of behavior can be observed in Fig. 4, which we will call normal and anomalous behavior, respectively:

(1) Normal behavior with a gradual reduction of SET resistance with increasing pulse height (see filled square and triangle symbols in Fig. 4). This is typically observed when the initial amorphous RESET resistance was >2 MΩ or when the initial RESET pulse length used was >50 ns.
(2) Anomalous behaviour with a sudden drop of the resistance to approximately 2 kΩ (see crosses and open circle symbols in Fig. 4). This is observed when the initial amorphous RESET resistance was <2 MΩ and the initial RESET pulse length was equal to 50 ns.

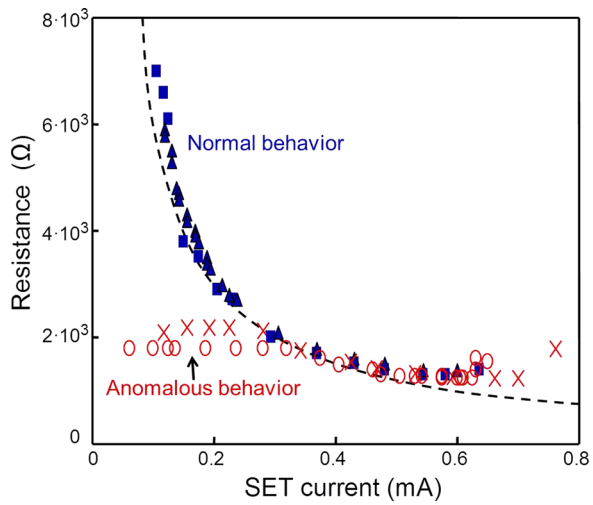

FIG. 4. Development of the SET resistance of various line cells as a function of pulses with gradually increasing SET current showing two types of behaviour which are described in detail in the main text. The different types of symbols indicate results of different cells, where the blue symbols (squares and triangles) hold for normal behaviour and the red symbols (circles and crosses) hold for anomalous behaviour. The black dashed line shows a hyperbolic relation between resistance and current which holds in case of gradual thickening of initially high-aspect ratio crystalline filaments. The data for normal behaviour are closely following the hyperbolic dependence.

In both cases, the current required for (partial) switching to the SET state is much lower than needed to uniformly heat the full cross-section of the line to 600–700 K. This suggests a kind of crystalline filament formation in the amorphous mark to explain the results of Fig. 4. Representative TEM images of line cells in the initial RESET state that gives rise to the two types of SET behaviour are presented in Figure 5, where the top image shows an example of a cell giving anomalous behaviour and the bottom one holds for normal behaviour.

The comparison between the amorphous mark observable in Fig. 2(b) with the ones observable in Fig. 5 indicates that a similar SET behavior is expected as in the top image of Fig. 5, i.e., anomalous behavior. Indeed, this is observed; also compare Fig. 3 with Fig. 4. In Fig. 3, the sudden drop is from 1.0 MΩ to 2.3 kΩ and then a small decrease to 2.0 kΩ. In Fig. 4, the sudden drop is to 2.0 kΩ and then a small decrease to about 1.4 kΩ. These results, including Fig. 2(c), seem to indicate that in case of the anomalous SET behavior, a kind of massive crystalline filament is formed that consumes most of the width of the amorphous mark explaining the sudden drop to low resistance values during the SET operation. This only leaves minor residual amorphous regions, which explains the small resistance decrease that is possible with increasing SET currents. The normal SET behavior should then occur with crystalline filament(s) having large aspect ratio between length and width. Only in this case a relatively high initial SET resistance of 7 kΩ is expected that can be still reduced gradually and largely to about 1.5 kΩ by a continuously increasing width of the crystalline filament(s) until the whole amorphous mark has been crystallized. Unfortunately, formation of these high aspect ratio crystalline filament(s) with their gradual lateral growth was not observed by us in any TEM image, also due to the altered thermal behavior of the sample due to removal of surrounding material for TEM sample preparation. This altered behavior suppresses the possibility to observe high aspect ratio crystalline filaments. Still, support for this scenario comes from the following simple model.

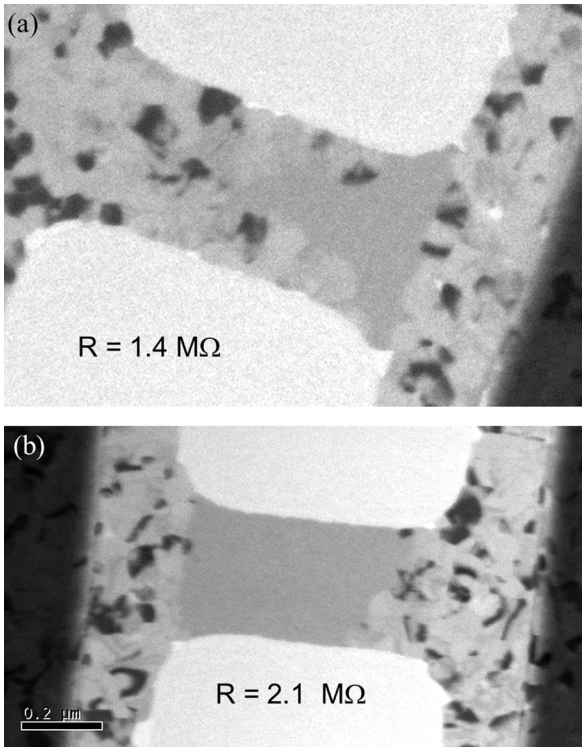

FIG. 5. TEM images of 700 nm long line cells in the RESET state showing on top a line cell with a small amorphous mark with nonuniform shape corresponding to a low resistance of 1.4 MΩ and at the bottom a line cell with a large amorphous mark with uniform filling of the line. Note that these FIB prepared TEM samples were not prepared according to a method that still allows electrical access to the line cells, but were produced according to the method described in Ref. 9.

We start by stating that the power density p_{cryst} required to crystallize a filament of length L and cross-sectional area A should be independent of A and can be written as

$$p_{cryst} = J^2\rho \tag{1}$$

with J the current density, which can be described by

$$J = \frac{I}{A} \tag{2}$$

with I the total current that is running through the line cell (which in principle only runs through the crystalline filament, because the amorphous surroundings have much higher resistance) and ρ the resistivity of the crystalline filament which can be described by

$$\rho = \frac{RA}{L}. \tag{3}$$

Now by extracting the cross-sectional area A from Eq. (3), substituting it in Eq. (2) and then plugging the result in Eq. (1) gives

$$p_{cryst} = \frac{I^2R^2}{\rho L^2}. \tag{4}$$

Because in our experiment the length of the crystalline filament is determined by the amorphous mark length and does not change in a first order approximation when increasing the SET current pulse and we also assume that the resistivity of the crystalline filament remains constant, then the result in Eq. (4) demonstrates that the product of the current I and the resistance R should be constant and thus indicates a hyperbolic behavior. Indeed, the black dashed line in Fig. 4, describing a hyperbolic behavior, matches the experimental data for the normal SET behavior rather well and thus suggests that the normal SET behavior occurs by formation of crystalline filaments which subsequently only grow in the lateral direction until the whole amorphous mark is crystallized. Thinning actual memory cells such that they can be observed in the TEM tends to shift the SET behavior towards the anomalous behavior, because due to the associated reduction in cooling rate the formation of high aspect ratio crystalline filaments is hampered in favor of more massive crystallization as we already observed in Fig. 2(c).

CONCLUSIONS

PRAM cells were processed in such a way that they could be observed in the TEM but still could be addressed and thus be switched and characterized electrically. A

drawback of the processing method used is that it was difficult to probe the cells, because the silicon was completely removed from the back also below the bond pads. The delicate membrane that remained after removal of the silicon was easily punctured by the probe needles. Still, interesting results have been obtained, where electrical properties could be related to the TEM images. It was found that crystallization initiates from a narrow channel with amorphous marks still present on both sides. The cell could be crystallized completely by applying higher energy SET pulses. Furthermore, it was found that the PRAM cell processed for TEM observation could not be brought to a resistance as high as unprocessed cells. This was related to re-crystallization of the molten region during the melt-quench phase. Since a lot of material, particularly a part of the electrical connection, was removed to allow for TEM observation, the heat dissipation is impacted. Therefore, it takes longer for the temperature of the active phase-change material to cool, leading to re-crystallization. This was clearly supported by the TEM observation and proves that more material was molten than the region that became amorphous.

Comparison with detailed electrical characterization showed two types of behavior for the relation between SET resistance and SET current when SET pulses with gradually increasing currents are used. The normal behavior holds for relatively long amorphous marks, showing a hyperbolic dependence between SET resistance and SET current, indicating a switching mechanism based on initially long and thin crystalline filaments which thicken gradually. The anomalous behavior we observed in our TEM switching experiment holds for relatively short amorphous marks, where initially directly a massive crystalline filament is formed that consumes most of the width of the amorphous mark only leaving minor residual amorphous regions at its edges. Despite our relatively thick TEM samples, the TEM sample preparation reduces the probability to observe high aspect ratio crystalline filaments. It shows that it is a great challenge to produce electrically switchable TEM specimen in which the memory cells behave the same as in their original better encapsulated state.

ACKNOWLEDGMENTS

The research was carried out under project number MC3.05241 in the framework of the Strategic Research program of the Materials innovation institute M2i. Financial support from the M2i is gratefully acknowledged.

[1]S. Hudgens and B. Johnson, MRS Bull. **29**, 829 (2004).
[2]M. H. R. Lankhorst, B. Ketelaars, and R. A. M. Wolters, Nature Mater. **4**, 347 (2005).
[3]S. Raoux, W. Welnic, and D. Ielmini, Chem. Rev. **110**, 240 (2010).
[4]G. W. Burr *et al.*, J. Vac. Sci. Technol. B **28**, 223 (2010).
[5]S. Meister, D. T. Schoen, M. A. Topinka, A. M. Minor, and Y. Cui, Nano Lett. **8**, 4562 (2008).
[6]Y. Jung, S.-W. Nam, and R. Agarwal, Nano Lett. **11**, 1364–1368 (2011).
[7]S. Meister, S.-B. Kim, J. J. Cha, H.-S. P. Wong, and Y. Cui, ACS Nano **2011**(5), 2742.
[8]S.-W. Nam and R. Agarwal, Science **336**, 1561 (2012).
[9]B. J. Kooi, J. L. M. Oosthoek, M. A. Verheijen, M. Kaiser, F. J. Jedema, and D. J. Gravesteijn, Phys. Status Solidi **249**, 1972 (2012).
[10]G. F. Zhou, Mater. Sci. Eng., A **304–306**, 73 (2001).
[11]S. Raoux, Ann. Rev. Mater. Res. **39**, 25 (2009).
[12]D. Tio Castro *et al.*, Tech. Dig. – Int. Electron Devices. Meet. **2007**, 315.
[13]F. J. Jedema, M. A. A. in't Zandt, and W. S. M. M. Ketelaars, Appl. Phys. Lett. **91**, 203509 (2007).
[14]L. Goux, D. Tio Castro, G. A. M. Hurkx, J. G. Lisoni, R. Delhougne., D. J. Gravesteijn, K. Attenborough, and D. J. Wouters, IEEE. Trans. Electron. Devices **56**, 354 (2009).
[15]F. Jedema, M. in't Zandt, R. Wolters, and D. Gravesteijn, Jpn. J. Appl. Phys., Part 1 **50**, 024102 (2011).
[16]J. L. M. Oosthoek, K. Attenborough, G. A. M. Hurkx, F. J. Jedema, D. J. Gravesteijn, and B. J. Kooi, J. Appl. Phys. **110**, 024505 (2011).
[17]J. L. M. Oosthoek, D. Krebs, M. Salinga, D. J. Gravesteijn, G. A. M. Hurkx, and B. J. Kooi, J. Appl. Phys. **112**, 084506 (2012).
[18]J. L. M. Oosthoek, B. J. Kooi, J. T. M. De Hosson, D. Gravesteijn, K. Attenborough, R. Wolters, and M. Verheijen, in *Proceedings of the E/PCOS Symppsium* (2009), p. 140.
[19]B. Rajendran *et al.*, IEEE Symp. VLSI Tech. **2008**, 96.
[20]C. Kim, D. M. Kang, T. Y. Lee, K. H. P. Kim, Y. S. Kang, J. Lee, S. W. Nam, K. B. Kim, and Y. Khang, Appl. Phys. Lett. **94**, 193504 (2009).
[21]D. M. Kang, D. Lee, H. M. Kim, S. W. Nam, M. H. Kwon, and K. B. Kim, Appl. Phys. Lett. **95**, 011904 (2009).
[22]S. W. Nam, D. Lee, M. H. Kwon, D. M. Kang, C. Kim, T. Y. Lee, S. Heo, Y. W. Park, K. Lim, H. S. Lee, J. S. Wi, K. W. Yi, Y. Khang, and K. B. Kim, Electrochem Solid State **12**, H155 (2009).
[23]T.-Y. Yang, I.-M. Park, B.-J. Kim, and Y.-C. Joo, Appl. Phys. Lett. **95**, 032104 (2009).
[24]T.-Y. Yang, J.-Y. Cho, Y.-J. Park, and Y.-C. Joo, Acta Mater. **60**, 2021 (2012).
[25]V. Weidenhof, I. Friedrich, S. Ziegler, and M. Wuttig, J. Appl. Phys. **86**, 5879 (1999).
[26]R. Pandian, B. J. Kooi, G. Palasantzas, J. T. M. De Hosson, and A. Pauza, Adv. Mater. **19**, 4431 (2007).
[27]R. E. Simpson, M. Krbal, P. Fons, A. V. Kolobov, J. Tominaga, T. Uruga, and H. Tanida, Nano Lett. **10**, 414 (2010).
[28]G. Eising, A. Pauza, and B. J. Kooi, Cryst. Growth Des. **13**, 220 (2013).
[29]D. Krebs, S. Raoux, C. T. Rettner, G. W. Burr, M. Salinga, and M. Wuttig, Appl. Phys. Lett. **95**, 082101 (2009).
[30]See supplementary material at http://dx.doi.org/10.1063/1.4908023 for experimental details including preparation of TEM specimen allowing *in situ* electrical switching and characterization.